

TAOK1 is associated with neurodevelopmental disorder and essential for neuronal maturation and cortical development

Geeske M. van Woerden^{1,2,3}  | Melanie Bos⁴  | Charlotte de Konink¹ | Ben Distel^{1,2,5}  | Rossella Avagliano Trezza¹  | Natasha E. Shur⁶ | Kristin Barañano⁷ | Sonal Mahida⁷ | Anna Chassevent⁷ | Allison Schreiber⁸ | Angelika L. Erwin⁸  | Karen W. Gripp⁹ | Fatima Rehman¹ | Saskia Brulleman¹ | Róisín McCormack¹  | Gwynna de Geus¹  | Louisa Kalsner¹⁰ | Arthur Sorlin^{11,12,13}  | Ange-Line Bruel^{11,12,13}  | David A. Koolen⁴ | Melissa K. Gabriel¹⁴ | Mari Rossi¹⁴ | David R. Fitzpatrick¹⁵ | Andrew O.M. Wilkie^{16,17}  | Eduardo Calpena¹⁶  | David Johnson¹⁷ | Alice Brooks³ | Marjon van Slegtenhorst³ | Julie Fleischer¹⁸ | Daniel Groepper¹⁸ | Kristin Lindstrom¹⁹ | A. Micheil Innes²⁰  | Allison Goodwin²¹ | Jennifer Humberson²² | Amanda Noyes²³ | Katherine G. Langley²³ | Aida Telegrafi²³ | Amy Blevins²³ | Jessica Hoffman²³ | Maria J. Guillen Sacoto²³ | Jane Juusola²³ | Kristin G. Monaghan²³ | Sumit Punj²³ | Marleen Simon²⁴ | Rolph Pfundt⁴ | Ype Elgersma^{1,2}  | Tjitske Kleefstra⁴

¹Department of Neuroscience, Erasmus MC, Rotterdam, The Netherlands²The ENCORE Expertise Center for Neurodevelopmental Disorders, Erasmus MC, Rotterdam, The Netherlands³Department of Clinical Genetics, Erasmus MC, Rotterdam, The Netherlands⁴Department of Human Genetics, Radboud University Medical Center, Donders Institute for Brain, Cognition and Behaviour, Nijmegen, The Netherlands⁵Department of Medical Biochemistry, Amsterdam UMC, University of Amsterdam, Amsterdam, The Netherlands⁶Division of Genetics and Metabolism, Rare Disease Institute, Children's National Medical Center, Washington, District of Columbia, USA⁷Department of Neurogenetics, Kennedy Krieger Institute, Baltimore, Maryland, USA⁸Genomic Medicine Institute, Cleveland Clinic, Cleveland, Ohio, USA⁹Division of Medical Genetics, Nemours/A.I. duPont Hospital for Children, Wilmington, Delaware, USA¹⁰Departments of Neurology and Pediatrics, Connecticut Children's Medical Center and University of Connecticut School of Medicine, Farmington, Connecticut, USA¹¹UMR1231 GAD, Inserm, Université Bourgogne-Franche Comté, Dijon, France¹²Unité Fonctionnelle Innovation en Diagnostic génomique des maladies rares, FHU-TRANSLAD, CHU Dijon Bourgogne, Dijon, France¹³Centre de Référence maladies rares «Anomalies du Développement et syndromes malformatifs», Centre de Génétique, FHU-TRANSLAD, CHU Dijon Bourgogne, Dijon, France¹⁴Department of Clinical Diagnostics, Ambry Genetics, Aliso Viejo, California, USA¹⁵MRC Human Genetics Unit, MRC IGMM, University of Edinburgh, Edinburgh, UK

Geeske M. van Woerden, Melanie Bos, Ype Elgersma and Tjitske Kleefstra contributed equally to this study.

This is an open access article under the terms of the Creative Commons Attribution-NonCommercial-NoDerivs License, which permits use and distribution in any medium, provided the original work is properly cited, the use is non-commercial and no modifications or adaptations are made.

© 2021 The Authors. *Human Mutation* published by Wiley Periodicals LLC.

¹⁶Clinical Genetics Group, MRC Weatherall Institute of Molecular Medicine, University of Oxford, Oxford, UK

¹⁷Oxford Craniofacial Unit, Oxford University Hospital NHS Foundation Trust, John Radcliffe Hospital, Oxford, UK

¹⁸Department of Pediatrics, SIU School of Medicine, Springfield, Illinois, USA

¹⁹Division of Genetics and Metabolism, Phoenix Children's Hospital, Phoenix, Arizona, USA

²⁰Department of Medical Genetics and Alberta Children's Hospital Research Institute, Cumming School of Medicine, University of Calgary, Calgary, Alberta, Canada

²¹VCU Medical Center, Clinical Genetics Services, Richmond, Virginia, USA

²²Division of Pediatric Genetics, Department of Pediatrics, University of Virginia Medical Center, Charlottesville, Virginia, USA

²³GeneDx, Gaithersburg, Maryland, USA

²⁴Department of Genetics, University Medical Center Utrecht, Utrecht, The Netherlands

Correspondence

Geeske M. van Woerden and Ype Elgersma, Department of Neuroscience, Erasmus MC, Dr. Molewaterplein 40, 3015 GD, Rotterdam, The Netherlands.

Email: g.vanwoerden@erasmusmc.nl and y.elgersma@erasmusmc.nl

Tjitske Kleefstra, Department of Human Genetics, Radboud University Medical Center, Donders Institute for Brain, Cognition and Behaviour, Nijmegen 6500 GA, Utrecht, The Netherlands.

Email: Tjitske.Kleefstra@radboudumc.nl

Funding information

NIHR, Oxford Biomedical Research Centre Programme; Nederlandse Organisatie voor Wetenschappelijk Onderzoek (ZonMW), Grant/Award Number: 91718310; Horizon 2020 Framework Programme, Grant/Award Number: 779257

Abstract

Thousand and one amino-acid kinase 1 (TAOK1) is a MAP3K protein kinase, regulating different mitogen-activated protein kinase pathways, thereby modulating a multitude of processes in the cell. Given the recent finding of TAOK1 involvement in neurodevelopmental disorders (NDDs), we investigated the role of TAOK1 in neuronal function and collected a cohort of 23 individuals with mostly *de novo* variants in *TAOK1* to further define the associated NDD. Here, we provide evidence for an important role for TAOK1 in neuronal function, showing that altered TAOK1 expression levels in the embryonic mouse brain affect neural migration *in vivo*, as well as neuronal maturation *in vitro*. The molecular spectrum of the identified TAOK1 variants comprises largely truncating and nonsense variants, but also missense variants, for which we provide evidence that they can have a loss of function or dominant-negative effect on TAOK1, expanding the potential underlying causative mechanisms resulting in NDD. Taken together, our data indicate that TAOK1 activity needs to be properly controlled for normal neuronal function and that TAOK1 dysregulation leads to a neurodevelopmental disorder mainly comprising similar facial features, developmental delay/intellectual disability and/or variable learning or behavioral problems, muscular hypotonia, infant feeding difficulties, and growth problems.

KEYWORDS

cortical development, functional genomics, *in utero* electroporation, neurodevelopmental disorders, TAOK1

1 | INTRODUCTION

Next-generation sequencing has led to rapid advances in understanding the genetic background for many neurodevelopmental disorders (NDDs). Indeed, genome sequencing (GS) or exome sequencing (ES) is now often used as diagnostic tools for unexplained NDDs, and the list of novel, defined syndromes has been expanding rapidly (Deciphering Developmental Disorders Study, 2017; Lelieveld et al., 2016; Wright et al., 2018). Here, we describe the identification of TAOK1 variants in patients with NDD, as identified by ES, and define the associated core phenotype.

Thousand and one amino-acid protein kinases (TAOKs) are part of the Ste20p protein kinase family and include TAOK1 (also called

PSK2 or MARKK), TAOK2 (also called PSK1), and TAOK3 (also called JNK [c-Jun NH2-terminal kinase]-inhibiting kinase). These kinases act upstream in the mitogen-activated protein kinase cascade, thereby regulating many cellular processes (Dan et al., 2001). Knockdown of *Tao1* in *Drosophila* (which is the only representative of the TAOK family in *Drosophila*) is shown to affect brain volume at larval stages (Poon et al., 2016) and results in early lethality, a smaller ventral nerve cord, and a reduced number of neuromuscular junction endings, implying a critical role of the TAOK family in *Drosophila* neurodevelopment (Dulovic-Mahlow et al., 2019). In the mammalian TAOK family, TAOK2 plays an important role in neurodevelopment as *Taok2* knockout mice show cognitive deficits as well as abnormal neural connectivity with shorter dendrites and fewer

spines on neurons in the prefrontal cortex (Richter et al., 2018). *TAOK2* has also been implicated in human neurodevelopment, as it is located at 16p11.2, a region associated with autism spectrum disorder (ASD) and schizophrenia (Pucilowska et al., 2015; L. A. Weiss et al., 2008). Indeed, patients with ASD harboring *de novo* variants in *TAOK2* were identified recently, and these variants affect *TAOK2* protein function, causing either loss-of-function (LoF) or a dominant-negative effect (Richter et al., 2018).

The role of *TAOK1* in neuronal function has been less well documented. *TAOK1* is a MAP3K protein kinase, which regulates the p38 as well as the JNK pathways either directly (Hutchison et al., 1998; Raman et al., 2007; Zihni et al., 2006) or indirectly through interleukin-17 (Z. Zhang et al., 2018). *TAOK1* is highly homologous to *TAOK2*, consisting of a catalytic domain, a substrate-binding domain, a spacer, and a tail (Timm et al., 2003). The major difference between the two kinases arises from the distinct tail domains, where *TAOK2* contains a microtubule-binding domain, which is absent in *TAOK1* (Zihni et al., 2006). *TAOK1* is involved in neurite outgrowth, axonal transport regulation, and in differentiating PC12 cells through the activation of PAR-1 (Timm et al., 2003). Additionally, human *TAOK1* was shown to be involved in mitogenesis by being an important regulator of checkpoint control, indicating a developmental role (Draviam et al., 2007). Human *TAOK1* is located on 17q11.2, close to *NF1* (Zihni et al., 2006). An individual with developmental delay, dysmorphic features, microcephaly, and short stature, was reported to harbor a *de novo* microdeletion at chromosome 17q11.2, resulting in haploinsufficiency of seven candidate genes, including *TAOK1* (Xie et al., 2016). In addition, direct evidence for *TAOK1* being a neurodevelopmental disorder gene surfaced through the identification of eight patients with NDD carrying *de novo* variants in *TAOK1* (Dulovic-Mahlow et al., 2019).

Here, we provide further evidence that *TAOK1* is involved in mammalian brain development by manipulating *TAOK1* expression during mouse brain development and describe the molecular and clinical data of 22 additional individuals carrying mutations affecting *TAOK1*.

2 | MATERIAL AND METHODS

2.1 | Patients

We collected the molecular and clinical features of 20 individuals with an intragenic *TAOK1* variant and three patients with a chromosomal deletion, including *TAOK1*. Most patients were included as the result of a collaboration facilitated by GeneMatcher (Sobreira et al., 2015) in which multiple clinical and research groups independently identified individuals with intellectual disability/developmental delay (ID/DD) or other related phenotypes with rare variations in *TAOK1*. Furthermore, a Pubmed search has been executed to find an additional case in which a small chromosome deletion involving *TAOK1* was thought to be causative for the patient's phenotype (Xie et al., 2016).

Clinical analysis of these patients was performed during regular consultations focusing on medical history, physical examination, and observational analysis of behavioral features. In all patients, exome sequencing and variant filtering were performed, according to the routine procedures at each institute (Farwell et al., 2014; Farwell Hagman et al., 2016; Retterer et al., 2015; Twigg et al., 2015; K. Weiss et al., 2016).

Informed consent to publish data was obtained from all patients, either as part of the diagnostic workflow or as part of a research study. Informed consent to publish clinical photographs was also obtained if applicable. Informed consent matched the local ethical guidelines.

2.2 | In silico modeling

For homology modeling, the protein sequence of *TAOK1* (NP_065842.1) was submitted to the I-TASSER protein structure prediction server (Yang & Zhang, 2015). For structural representation, the model with the highest confidence (C-score) and topological similarity (Tm-score) was used. Structural representations were made with the PyMOL Molecular Graphics System, Version 2.0 Schrödinger, LLC.

2.3 | Constructs

The complementary DNA (cDNA) sequence from human *TAOK1*^{WT} (NM_020791.2) was obtained from a human brain cDNA library by polymerase chain reaction (PCR) (Phusion high fidelity; Thermo Fisher Scientific) using the following primers: Fw 5'-GGCGCGCTCCATGGGCCATCAACTAACAGAGCAGG-3' and Rev 5'-TTAATTAAGCGGCCGCTTATGTATAAGACATGTGTGACCC-3' and cloned into our dual promoter expression vector containing the CAGG promoter to drive transcription of the gene of interest and a separate PGK promoter for transcription of the *tdTomato* gene (Küry et al., 2017; Proietti Onori et al., 2018; Reijnders et al., 2017). The single-nucleotide point mutation was introduced by PCR (Phusion high fidelity, Thermo Fisher Scientific) using the following primers: *TAOK1*-c.449G>T (p.Arg150Ile), Fw 5'-CA TTCTACTACTATGATTCATATAGATATCAAAGCAGGAAATATC-3' and Rev 5'-GATATTTCTGCTTTGATATCTATGAATCATAGTATGAG AATG-3'. *TAOK1*-c.500T>G (p.Leu167Arg), Fw 5'-CAGGCCAGGTGAAA CGTGCTGACTTTGGCTC-3' and Rev 5'-GAGCCAAAGTCAGCACG TTTACCTGGCCTG-3'. *TAOK1*-c.691A>G (p.Met231Val), Fw 5'-CCTT TATTAATATGAATGCAGTGAGTGCCTTATATCACATAG-3' and Rev 5'-CTATGTGATATAAGGCACTCACTGCATTCATATTAATAAAG G-3'. *TAOK1*-c.943C>T (p.Leu315Phe), Fw 5'-GCAGTATCGAAAGA TGAAGAAATTCCTTTCCAGGAGGCACATAA-3' and Rev 5'-TTATGT GCCTCCTGGAAAAGGAATTTCTTCATCTTTCCGATACTGC-3'. *TAOK1*-c. 1643T>C (p.Leu548Pro), Fw 5'-CCCAACAGAAGAAAGAACCGAATAG TTTTCTCGAGTC-3' and Rev 5'-GACTCGAGAAAACATTCGGTTCT TTCTTCTGTTGGG-3'. The truncated *TAOK1* was also generated by PCR (Phusion high fidelity, Thermo Fisher Scientific) using the following

primers: *TAOK1*-c.2442* (p.Tyr815Ter), Fw 5'-GAATCCGGCGCCACCATGCCATCAACTAACAGAGC-3' and Rev 5'-GAATCCTTAA TTAATTACGCATTC AACAGCTCCAGTTCC-3'. For all the in vivo and in vitro experiments, the dual promoter expression vector without a gene inserted was used as control (control vector). Short hairpin RNA (shRNA) constructs were obtained from the MISSION shRNA library for mouse genomes of Sigma Life Sciences and The RNAi Consortium. For knock-down of *TAOK1* we used three different shRNA plasmids, each targeting a different sequence: (1) GCCATTTACAAGTGGAAATAA, (2) CCATCT CAACACTATTCAGAA, and (3) GACTCGAAAGTTAGCCATCTT. The control shRNA plasmid is the MISSION nontarget shRNA control vector: CAACAAGATGAAGAGCACCAA.

2.4 | Mice

For the neuronal cultures, FvB/NHsD females were crossed with FvB/NHsD males (both ordered at 8- to 10-weeks old from Envigo). For the in utero electroporation, female FvB/NHsD (Envigo) were crossed with male C57Bl6/J (ordered at 8- to 10-weeks old from Charles River). All mice were kept group-housed in IVC cages (Sealsafe 1145T; Tecniplast) with bedding material (Lignocel BK 8/15 from Rettenmayer) on a 12-h light/dark cycle at 21°C ± 1°C, humidity at 40%–70% and with food pellets (801727CRM(P) from Special Dietary Service) and water available ad libitum. All animal experiments were conducted in accordance with the European Commission Council Directive 2010/63/EU (CCD approval AVD101002017893).

2.5 | HEK-293T cell transfections

To test the expression levels of the *TAOK1* constructs, we chose HEK-293T cells, a cell line easy to transfect and culture. These cells were not authenticated. HEK-293T cells were cultured in DMEM/10% fetal calf serum/1% penicillin/streptomycin in six-well plates and transfected when 60% confluent with the following DNA constructs: Control vector, *TAOK1*^{WT}, *TAOK1*^{Arg150Ile}, *TAOK1*^{Leu167Arg}, *TAOK1*^{Met231Val}, *TAOK1*^{Leu315Phe}, or *TAOK1*^{Leu548Pro} (3 µg per six-well dish). Transfection of the plasmids was done using polyethyleneimine according to the manufacturer's instructions (Sigma). After 4–6 h of transfection, the medium was changed to reduce toxicity. Transfected cells were then used for Western blot analysis.

2.6 | Western blot analysis

Two to three days after transfection, HEK-293T cells were harvested and homogenized in lysis buffer (10 mM Tris-HCl 6.8, 2.5% sodium dodecyl sulfate, 2 mM EDTA), containing protease inhibitor cocktail (#P8340; Sigma), phosphatase inhibitor cocktail 2 (#P5726; Sigma), and phosphatase inhibitor cocktail 3 (#P0044; Sigma). Protein concentration was determined using the bicinchoninic acid protein assay

kit (Pierce), after which lysate concentrations were adjusted to 1 mg/ml. Western blots were probed with primary antibodies against *TAOK1* (STJ95247, 1:1000; St. John Lab) and red fluorescent protein (RFP) (#600401379, 1:2000; Rockland; used to detect tdTomato) and secondary antibodies (goat anti-mouse (#926-32210) and goat anti-rabbit (#926-68021), all 1:15,000, LI-COR). Blots were quantified using LI-COR Odyssey Scanner and Odyssey 3.0 software. The intensity of the full-length *TAOK1* protein was measured. To assess the expression levels of *TAOK1* in different conditions, normalization was done against tdTomato (RFP signal).

2.7 | Primary hippocampal cultures

Primary hippocampal and cortical neuronal cultures were prepared from FvB/NHsD wild-type mice according to the procedure described previously (Goslin & Banker, 1991). Briefly, hippocampi were isolated from the brains of E16.5 embryos and collected altogether in 10 ml of neurobasal medium (NB; Gibco) on ice. The samples were incubated in prewarmed trypsin/EDTA solution (Invitrogen) at 37°C for 20 min, and dissociated using a 5-ml pipette in 1.5-ml NB medium supplemented with 2% B27, 1% penicillin/streptomycin, and 1% glutamax (Invitrogen). Following dissociation, neurons were plated in a small drop on poly-D-lysine (25 mg/ml, Sigma)-coated 15-mm glass coverslips at a density of 1 × 10⁶ cells per coverslip in 12-well plates containing 1 ml of supplemented NB for each coverslip. The plates were stored at 37°C/5% CO₂ until the day of the transfection.

2.8 | Neuronal transfection and immunocytochemistry

Neurons were transfected after 3 days in vitro (DIV) with the following DNA constructs: control vector (1.8 µg per coverslip), *TAOK1*^{WT}, *TAOK1*^{Arg150Ile}, *TAOK1*^{Leu167Arg}, *TAOK1*^{Met231Val}, *TAOK1*^{Leu315Phe} or *TAOK1*^{Leu548Pro} (all 2.5 µg per coverslip), or cotransfected with either shRNAs against *Taok1* (single or pool of all together) or scramble shRNA and RFP plasmid (Addgene) (1 µg per construct per coverslip). Lipofectamine 2000 was used to transfect neurons, according to the manufacturer's instructions (Invitrogen). For the neuronal morphology analysis, neurons were fixed 5 days posttransfection with 4% paraformaldehyde (PFA)/10% sucrose and incubated overnight at 4°C with MAP2 (1:500, #188004; Synaptic System) and *TAOK1* (STJ95247, 1:100; St. John Lab) in GDB buffer (0.2% bovine serum albumin, 0.8 M NaCl, 0.5% Triton X-100, 30 mM phosphate buffer, pH 7.4). The next day the neurons were incubated for 1 h in the anti-guinea-pig-Alexa647 (#706-605-148) conjugated secondary antibody (1:200; Jackson ImmunoResearch). Slides were mounted using Mowiol-DABCO (Sigma) mounting medium. Confocal images were acquired using an LSM700 confocal microscope (Zeiss).

For the analysis of the neuronal transfections, at least 10 confocal images (×20 objective, 0.5 zoom, 1024 × 1024 pixels) of different transfected neurons (identified by the red staining from the

tdTomato) were taken from each coverslip for each experiment with at least two independent replications. For the analysis of the intensity of TAOK1 signal and neuronal morphology, the ImageJ software was used. For the intensity, the fluorescent signal of endogenous TAOK1 was measured in somas of transfected and five nontransfected surrounding neurons. The intensity of the transfected neuron was then divided over the nontransfected neurons. For neuronal morphology, the dendrites with their branches were measured using the NeuronJ plugin of ImageJ. Total neurite length was measured and analyzed and for the arborization, the number of branching of each primary neurite (=coming directly from the soma) was counted and analyzed. All values were normalized against the mean value for each parameter of the control (empty vector control). The analysis was done by an experimenter blinded for the transfection conditions.

2.9 | In-utero electroporation

The procedure was performed as described previously (Proietti Onori et al., 2018). In short, pregnant FvB/NHsd mice at E14.5 of gestation were anesthetized, and the uterus was exposed. The DNA construct (1.5–3 $\mu\text{g}/\mu\text{l}$) was diluted in fast green (0.05%) and injected in the lateral ventricle of the embryos while still *in the uterus*, using a glass pipette controlled by a Picospritzer[®] III device. To ensure the proper electroporation of the injected DNA constructs (1–2 μl) into the progenitor cells, five electrical square pulses of 45 V with a duration of 50 ms per pulse and 150-ms interpulse interval were delivered using tweezer-type electrodes connected to a pulse generator (ECM 830, BTX Harvard Apparatus). The electrodes were placed in such a way that the positive pole was targeting the developing somatosensory cortex. The following plasmids were injected: control vector, *TAOK1^{WT}*, *TAOK1^{Arg150Ile}*, *TAOK1^{Leu167Arg}*, *TAOK1^{Met231Val}*, *TAOK1^{Leu315Phe}*, or *TAOK1^{Leu548Pro}* or for knockdown experiments: A pool of the *Taok1* shRNAs with an RFP plasmid (Addgene) or the control shRNA with an RFP plasmid. To make sure the effect on migration was specific for the knockdown of *Taok1*, the single shRNAs were also tested individually and resulted in similar migration deficits (data not shown). After birth, pups (M/F) were sacrificed at P1 or P7 for histochemical processing.

2.10 | Immunohistochemistry

Mice were deeply anesthetized with an overdose of nembutal and transcardially perfused with 4% paraformaldehyde (PFA). Brains were extracted and post-fixed in 4% PFA. Brains were then embedded in gelatin and cryoprotected in 30% sucrose in 0.1 M phosphate buffer (PB), frozen on dry ice, and sectioned using a freezing microtome (40–50- μm thick). Free-floating coronal sections were washed in PBS and blocked in PBS containing 10% normal horse serum (NHS) and 0.5% Triton X-100 for 1 h at ambient temperature. Afterward, slices were incubated with primary antibody RFP

(#600401379, 1:2000; Rockland), diluted in PBS containing 2% NHS, 0.5% Triton X-100, at 4°C for 48–72 h. Slices were washed three times with PBS and the secondary antibody was added (Cy3 donkey-anti-rabbit, 1:400; Jackson ImmunoResearch) diluted in PBS containing 2% NHS, 0.5% Triton-X 100. Finally, the slices were counterstained with 4',6-diamidino-2-phenylindole solution (1:10,000; Invitrogen) before being mounted with Mowiol on the glass. Overview images of the coronal sections were acquired by tile scan imaging using an LSM700 confocal microscope (Zeiss) with a $\times 10$ objective.

Neuronal migration analysis was performed using confocal images ($\times 10$ objective, 0.5 zoom, 1024 \times 1024 pixels) obtained from two to three nonconsecutive sections from at least three successfully targeted animals per plasmid, as previously described (Küry et al., 2017; Proietti Onori et al., 2018; Reijnders et al., 2017). Briefly, images were rotated to correctly position the cortical layers, and the number of cells in different layers were counted using ImageJ (Analyze Particles option). Cortical areas from the pia to the ventricle were divided into 10 equally sized bins and the percentage of tdTomato-positive cells per bin was counted systematically.

2.11 | Statistical analysis

All data were assumed to be normally distributed. Statistical difference between the conditions for the *in vitro* and *in vivo* overexpression experiments was determined using one-way analysis of variance (ANOVA) followed by Dunnett's posthoc test for multiple comparisons and for the knockdown *in vivo* experiments using the two-tailed unpaired *t* test (dual comparison). For the western blot analysis, a two-tailed unpaired *t* test was used (dual comparison). Neuronal migration was analyzed based on the proportion of electroporated cell targeted to the cortical plate at P1 (defined as the most proximal 40% of the dorsoventral distance between the pia and ventricle [first 4 of 10 equally spaced bins]) or to layer 2/3 of the somatosensory cortex, defined as the proximal 30% of the dorsoventral distance between the proximal 10% of the cortex (assumed to represent layer 1) and ventricle (bin 2–4 of equally spaced bins). On the basis of our previous neuronal morphology analyses (Proietti Onori et al., 2018), we performed two replicates of a minimum of 10 neurons per condition. For neuronal migration analyses, we used a minimum of three targeted pups per condition. For the western blot analysis, we used at least three replicates.

3 | RESULTS

3.1 | TAOK1 plays an important role in cortical development

In utero electroporation in mice or rats is a valuable technique to study the role of specific proteins in neuronal function as an impaired neuronal function can result in abnormal cortical migration, a key

aspect of neurodevelopment (Saito & Nakatsuji, 2001; Tabata & Nakajima, 2001; Taniguchi et al., 2012). Hence, we used this technique to assess whether loss of TAOK1 would affect neuronal migration in vivo. First, we assessed the level of shRNA-mediated knockdown of mouse *Taok1* in neurons, using primary hippocampal culture in vitro as the antibody for TAOK1 did not work well on slices. We found, on average 35% reduction in TAOK1 immunofluorescence intensity for both the single shRNAs and the pooled conditions (Figures S1A and S1B).

We performed the in utero electroporation in mouse embryos at embryonic day 14.5, a well-established time in murine fetal development when neural progenitor cells divide to give rise to immature neurons that will migrate to their final destination within the cortical plate, which will form the cerebral cortex layer 2/3. We found that shRNA-mediated knockdown of *Taok1* (using a pool of three different shRNAs specifically targeting *Taok1*) at this time resulted in a clear migration deficit of the neurons coming from the transfected neural progenitor cells, with significantly fewer transfected cells reaching the cortical plate (CP) at postnatal day 1 (P1) compared to control (scramble shRNA) condition (70% vs. 90% respectively; $t[23]=4.21$, $p=.0003$, unpaired Student's *t* test, Figure 1a,b).

This migration deficit persists at P7 when only 75% of the targeted neurons were present in layer 2 of 3 of the somatosensory cortex compared to 95% in control conditions ($t[15]=2.84$, $p=.0124$, unpaired Student's *t* test, Figure 1c,d). Similar migration deficits were found when the shRNAs were tested separately, confirming their specificity (Figure S1C-E). Together these results indicate that TAOK1 plays a critical role in neuronal function and that reduction of TAOK1 levels results in impaired brain development.

3.2 | Phenotypic characterization of the variants found in TAOK1

Nineteen unrelated individuals with variants affecting TAOK1 were identified, which were heterozygous for a missense variant ($n=5$), premature stop variant ($n=7$), indel ($n=4$), or canonical splice site variant ($n=3$) (Tables 1 and S1). In addition, four individuals (individuals 18, 21, 22, and 23) carried a chromosomal microdeletion ranging in size from 807 bp to 2 Mb, of which patient 23 was previously published (Xie et al., 2016). The deletion found in individual 22 was inherited from a parent with a history of cognitive

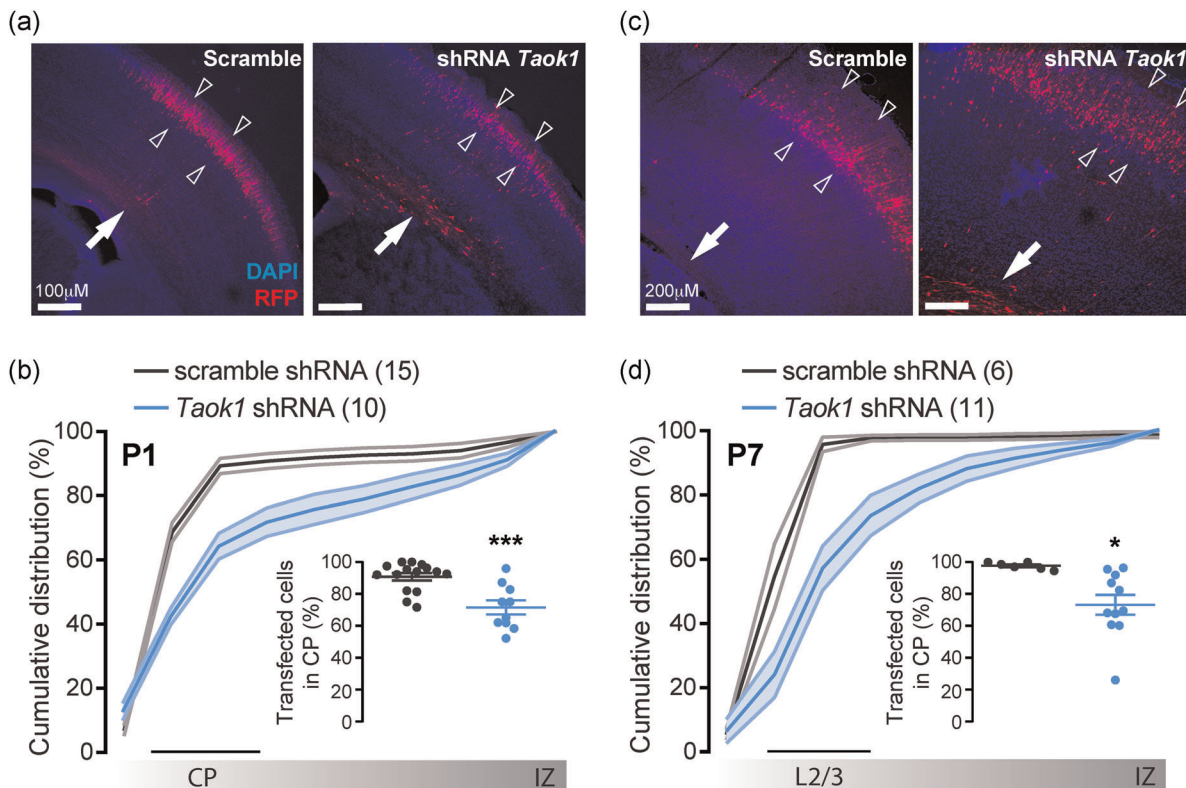


FIGURE 1 Knockdown of *Taok1* by in utero electroporation at embryonic day 14.5 results in a severe migration deficit. (a) Representative images from postnatal day 1 brain, showing the transfected cells (mRFP+) from the subventricular zone (SVZ; indicated by the arrow) to the cortical plate (CP; indicated by the arrowheads). (b) Cumulative distribution of the transfected neurons at P1 from the cortical plate (CP) to the intermediate zone (IZ). Inset, percentage of neurons reaching the superficial layers of the cortex (sum of bins 1 through 4). (c) Representative images from postnatal Day 7 brains, showing the transfected cells (mRFP+) from the SVZ to the cerebral cortex layer 2/3 (indicated by the arrowheads). (d) Cumulative distribution of the transfected neurons from layer 2/3 to the IZ. Inset, percentage of neurons reaching layer 2/3 of the cortex (sum of bins 2-4). Data are presented as mean \pm SEM. Numbers between brackets indicate the number of images analyzed for each condition. TAOK1, thousand and one amino-acid kinase 1; SEM, standard error of the means. *** $p < .001$

TABLE 1 Overview of the variants identified

Patient	Gender and age	Chromosome position (GRCh37)	cDNA change (NM_020791.2)	Amino acid change	Inheritance	Heterozygous/ Homozygous
Patient 1	Male, 5 years	chr17:g.27861216del	c.242del	p.Tyr815Ilefs*31	De novo	Heterozygous
Patient 2	Male, 9 years	chr17:g.27818884dup	c.831+1dupG	p.?	De novo	Heterozygous
Patient 3	Male, 8 years	chr17:g.27837949T>C	c.1643 T>C	p.Leu548Pro	De novo	Heterozygous
Patient 4	Female, 14 years	chr17:g.27822746dup	c.999+1dupG	p.?	De novo	Heterozygous
Patient 5	Male, 14 years	chr17:g.27844585C>T	c.1819 C>T	p.Gln607Ter	De novo	Heterozygous
Patient 6	Female, 2 years and 6 months	chr17:g.27818877_27818878insCT	c.825_826insCT	p.Lys277Ter	De novo	Heterozygous
Patient 7	Male, 6 years	chr17:g.27816684G>T	c.658G>T	p.Glu220Ter	Maternal, familial NDD	Heterozygous
Patient 8	Male, 20 years	chr17:g.27849514C>T	c.2125C>T	p.Arg709Ter	Paternal	Heterozygous
Patient 9	Male, 2 years	chr17:g.27805365G>T	c.449G>T	p.Arg150Ile	De novo	Heterozygous
Patient 10	Male, 17 years	chr17:g.27807436T>G	c.500T>G	p.Leu167Arg	De novo	Heterozygous
Patient 11	Male, 3 years	chr17:g.27849472C>T	c.2083C>T	p.Arg695Ter	De novo	Heterozygous
Patient 12	Female, 3 years	chr17:g.27805366G>C	c.449+1G>C	p.?	De novo	Heterozygous
Patient 13	Female, 1 year and 11 months	chr17:g.27805309dup	c.393dupT	p.Thr132Tyrfs*19	De novo	Heterozygous
Patient 14	Male, 5 years	chr17:g.27849493C>T	c.2104C>T	p.Arg702Ter	Unknown	Heterozygous
Patient 15	Male, 6 years	chr17:g.27822689C>T	c.943C>T	p.Leu315Phe	De novo	Heterozygous
Patient 16	Male, 10 years	chr17:g.27829690delA	c.1287delA	p.Lys429Asnfs*42	De novo	Heterozygous
Patient 17	Female, 1 year and 8 months	chr17:g.27802715_27802716del	c.232_233delAA	Lys78Valfs*20	De novo	Heterozygous
Patient 18	Male, 10 years	chr17:g.27848992_27849799del	c.1909-306_2148+262del	p.?(exon 17 deletion)	De novo	Heterozygous
Patient 19	Female, 21 years	chr17:g.27816717A>G	c.691 A>G	p.Met231Val	Unknown	Heterozygous
Patient 20	Female, 1 year and 2 months	chr17:g.27844579C>T	c.1813C>T	p.Arg605Ter	Unknown	Heterozygous
Patient 21	Female, 7 years	del17q11.2,27.08-29.08 Mb x 1	2 MB		N/A	Heterozygous
Patient 22	Male, 6 years	del chr17:27,670,438-27,934,287 x 1	264 kb		Maternally inherited (ID in parents)	Heterozygous
Patient 23	Female, 1 year and 9 months	del chr17:27,064,286-28,761,847 x 1	1.69 MB		De novo	N/A

Note: p. ? indicates that the effect on protein is unknown.

Abbreviations: cDNA, complementary DNA; ID, intellectual disability; NDD, neurodevelopmental disorder; N/A, not assessed.

impairment. For individuals 14, 19, and 20, no parental genotype data were available, so inheritance could not be determined. Two single nucleotide variants were inherited (individual 7 and 8). The variant found in individual 7 was inherited maternally. Although for the mother, no formal IQ was known, she was unable to follow conventional school. Moreover, there is a clear familial context of delayed development. The half-brother (maternal side) had an IQ of 72 and a grand-uncle (maternal side) was known with ID, so the *TAOK1* variant could potentially further segregate in this family. The variant found in individual 8 was paternally inherited. Here, although the father has symptoms of autism, he was never formally diagnosed or assessed for neurodevelopmental issues. This variant predicts a premature stop and is present once out of 251344 alleles in gnomAD (<https://gnomad.broadinstitute.org/>). All other variants in *TAOK1* identified in our cohort occurred de novo. There were additional de novo variants reported in our cohort in 11 different genes (Table S1; individuals 1, 7, 9, 10, 11, 17, 19, and 20). The de novo *ZEB2* variant in patient 10 is considered to be likely pathogenic and probably contributing to the phenotype, although the patient does not have clinically suspected Mowat-Wilson syndrome. The other de novo variants are of uncertain significance. Though unlikely, we cannot fully exclude a potential effect on the phenotypes of the respective patients.

We compiled the clinical data and compared that with the clinical data that have been reported previously (Dulovic-Mahlow et al., 2019) (Tables 2 and S1). This reveals that the collective features present in the majority of individuals that define the core clinical picture of the *TAOK1*-associated syndrome are: Varying degrees of ID/DD, neonatal feeding difficulties, overlapping facial

features, behavior problems, hypotonia, and joint hypermobility. Similar facial features observed comprise frontal bossing, downslanting palpebral fissures, long philtrum, and bulbous nasal tip (Figure 2a). Of note, patient 11 presented with multisuture craniosynostosis, which may have been related to prenatal ventriculomegaly and macrocephaly, causing the fetal head to be stuck in the pelvis. Some patients were too young to establish a formal diagnosis of ID, and for three individuals (patients 5, 8, and 15) no ID was present. Therefore, the cognitive phenotype might be very mild and could explain the presence of two vertical transmissions (patients 7 and 8) and presence in gnomAD of the variant in individual 8.

Microdeletions in the 17q11.2 region often encompass the *NF1* gene (Kehrer-Sawatzki et al., 2017). The microdeletions presented here, however, are proximally located to this more common deleted region. Previously, a novel de novo deletion at 17q11.2 adjacent to the *NF1* gene was reported in an individual with developmental delay, short stature, postnatal microcephaly, underweight, and dysmorphic features, including flat facial profile, dolichocephaly, hypertelorism, short philtrum, flat nasal bridge, and posteriorly rotated and low set ears. Chromosomal microarray analysis revealed a 1.69 Mb de novo deletion at 17q11.2 adjacent to *NF1* gene, which involved 43 RefSeq genes. We included this information in Table 1 (individual 23). The authors compared in their study the proband to three other cases with overlapping small deletions from databases (Xie et al., 2016). On the basis of their findings, they hypothesized that *TAOK1* might be involved in the developmental delay and microcephaly in their patient. However, the information we collected in our study from the individuals with *TAOK1* variants and the two individuals with overlapping microdeletions indicate that

Parameter	Frequency	Previous ^a	Total (%)
Delivery			
C-section	5/20	N/R	5/20 (25)
Growth			
Small stature (height for age <2.0 SD)	4/20	N/R	4/20 (20)
Overweight (weight for height >2.0 SD)	6/20	N/R	6/20 (30)
Macrocephaly (>2.0 SD)	7/18	3/8	10/26 (38)
Neurodevelopmental			
Global developmental delay	18/20	6/8	24/28 (86)
Intellectual disability	14/20	4/8	18/28 (64)
Behavior problems	12/20	2/8 ^b	14/28 (50)
Hypotonia	10/20	6/8	16/28 (57)
Gastrointestinal			
Neonatal feeding difficulties	9/18	N/R	9/18 (50)
Musculoskeletal			
Joint hypermobility	6/20	2/8	8/28 (29)
Recurrent ear/airway infections	6/18	N/R	6/18 (33)

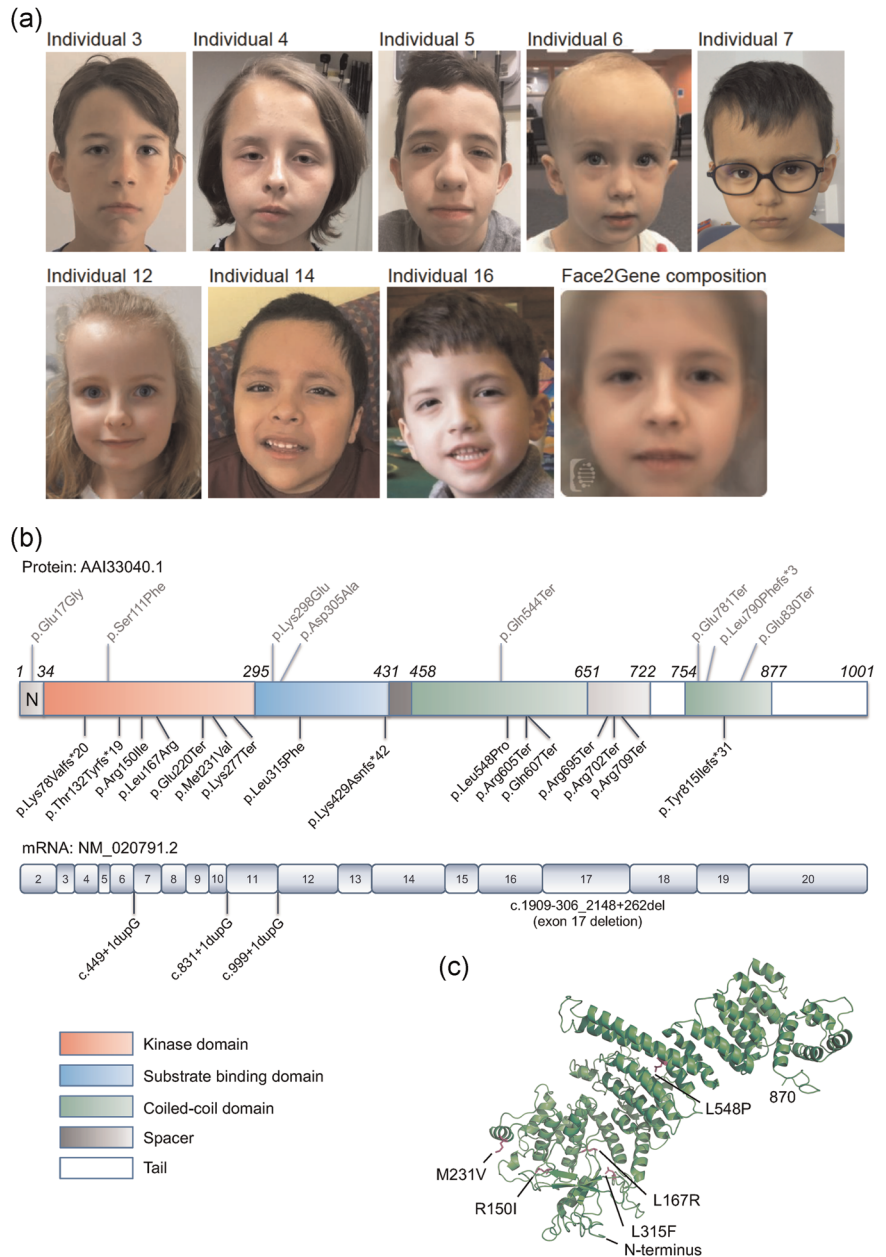
Abbreviations: N/R, not reported; *TAOK1*, thousand and one amino-acid kinase 1.

^aDulovic-Mahlow et al. (2019).

^bAttention deficit hyperactivity disorder (ADHD) and short attention span.

TABLE 2 Summary of clinical features found in the cohort of 20 individuals with *TAOK1* variants

FIGURE 2 Facial features of patients with de novo variants in thousand and one amino acid kinase 1 (TAOK1) and schematic overview of TAOK1 showing the location of the variants. (a) Facial profiles of seven unrelated patients and their facial composite created by the research tool of the Face2Gene application (FDNA Inc.), using the DeepGestalt algorithm (Gurovich et al., 2019). The facial features suggestive for the TAOK1-associated disorder include high forehead/ frontal bossing (individuals 4, 5, 6, 7, and 12), downslanting palpebral fissures (individuals 3, 4, 5, 14, and 16), long and/or pronounced philtrum, small chin (6, 7, and 12) and a bulbous nose (individuals 4, 5, 6, 7, and 12). (b) Schematic overview of the protein domain organization (top) and the corresponding messenger RNA structure (bottom) of TAOK1, with on top in gray the localization of the variants found previously (Dulovic-Mahlow et al., 2019), and below in black the localization of the novel variants identified here. (c) Structure of the TAOK1 protein from the N-terminal to amino acid 870, showing the localization of four of the missense variants (TAOK1^{Arg150Ile}, TAOK1^{Leu167Arg}, TAOK1^{Met231Val}, TAOK1^{Leu315Phe}, and TAOK1^{Leu548Pro}) identified here



microcephaly is not likely caused by loss of TAOK1, as the patients concerned have either occipitofrontal circumference in the normal range or above.

TAOK1 consists of a kinase domain in the N-terminal region (amino acids 34–295), a substrate-binding domain (SBD, amino acids 296–431), a spacer, and a tail, both containing a coiled-coil domain (CC). There is a high overall amino acid sequence conservation (~80% identity) between the human TAOK1 and TAOK1 from different vertebrate classes (Figure S2), with the least conserved part being the C-terminal region. Of the missense variants found in our cohort, two were located in the kinase domain, one in the SBD, and one in the first CC domain, all of which involved strictly conserved residues (Figure S2). Of the premature stop and indel variants, three were located in the kinase domain, one in the SBD, two in the CC, and three in the spacer (Figure 2b, top), indicating no real hotspot for

variants within the protein. The same applies to the variants found in the previous study (Dulovic-Mahlow et al., 2019) (Figure 2b, top, variants indicated in gray).

3.3 | Functional assessment of TAOK1 variants

Consistent with the finding that reduced TAOK1 levels affect neuronal function, the majority of the identified variants are predicted to cause a premature stop, indicating haploinsufficiency as the underlying molecular mechanism for the NDD, as was also shown previously (Dulovic-Mahlow et al., 2019). However, for the missense variants, the effect on protein function is less predictable. All missense variants are localized in highly conserved residues, with the identical amino acid sequence comparing human, mouse, rat, frog,

chicken, and zebrafish (Figure S2). In silico prediction of the variants using different prediction tools revealed that depending on the prediction tool used, the variants are damaging, likely damaging, or benign, hence, of unknown significance. Besides the variable outcomes obtained by these tools, they also do not address whether a missense variant causes an LoF or a gain of function (GoF). Therefore, we tested the effect of the TAOK1 missense variants on protein function. One of the variants, TAOK1^{Leu548Pro}, is predicted to be located in an alpha-helix structure in the protein (Figure 2c) and proline is in general considered to perturb the alpha-helix; hence, this variant could affect protein stability. To test the stability of the protein in the presence of different variants, HEK-293T cells were transfected with different constructs and the protein levels were assessed. Surprisingly, Western blot analysis revealed significantly reduced protein expression for two of the TAOK1 variants, predicted

to be located in a linker region in the kinase domain of the protein (TAOK1^{Arg150Ile} and TAOK1^{Leu167Arg}), whereas the TAOK1^{Leu548Pro} variant instead showed significantly higher protein level compared to TAOK1^{WT}, indicating that this variant does not cause intrinsic instability of the protein. The variants TAOK1^{Met231Val} and TAOK1^{Leu315Phe} did not alter the expression levels compared to TAOK1^{WT} (Figure 3a, one-way ANOVA, $F[5,66]=14.35$, $p < .0001$; TAOK1^{WT} vs. TAOK1^{Arg150Ile}, $p = .0029$; TAOK1^{WT} vs. TAOK1^{Leu167Arg}, $p = .0019$; TAOK1^{WT} vs. TAOK1^{Met231Val}, $p = .13$; TAOK1^{WT} vs. TAOK1^{Leu315Phe}, $p = .32$; TAOK1^{WT} vs. TAOK1^{Leu548Pro}, $p = .0029$, Dunnett's multiple comparison test).

Having established the effect of the variants at the protein level, we continued testing whether the variants behaved differently from TAOK1^{WT} in in vitro and in vivo assays to assess their pathogenicity. For the in vitro assay, mouse primary hippocampal neurons were

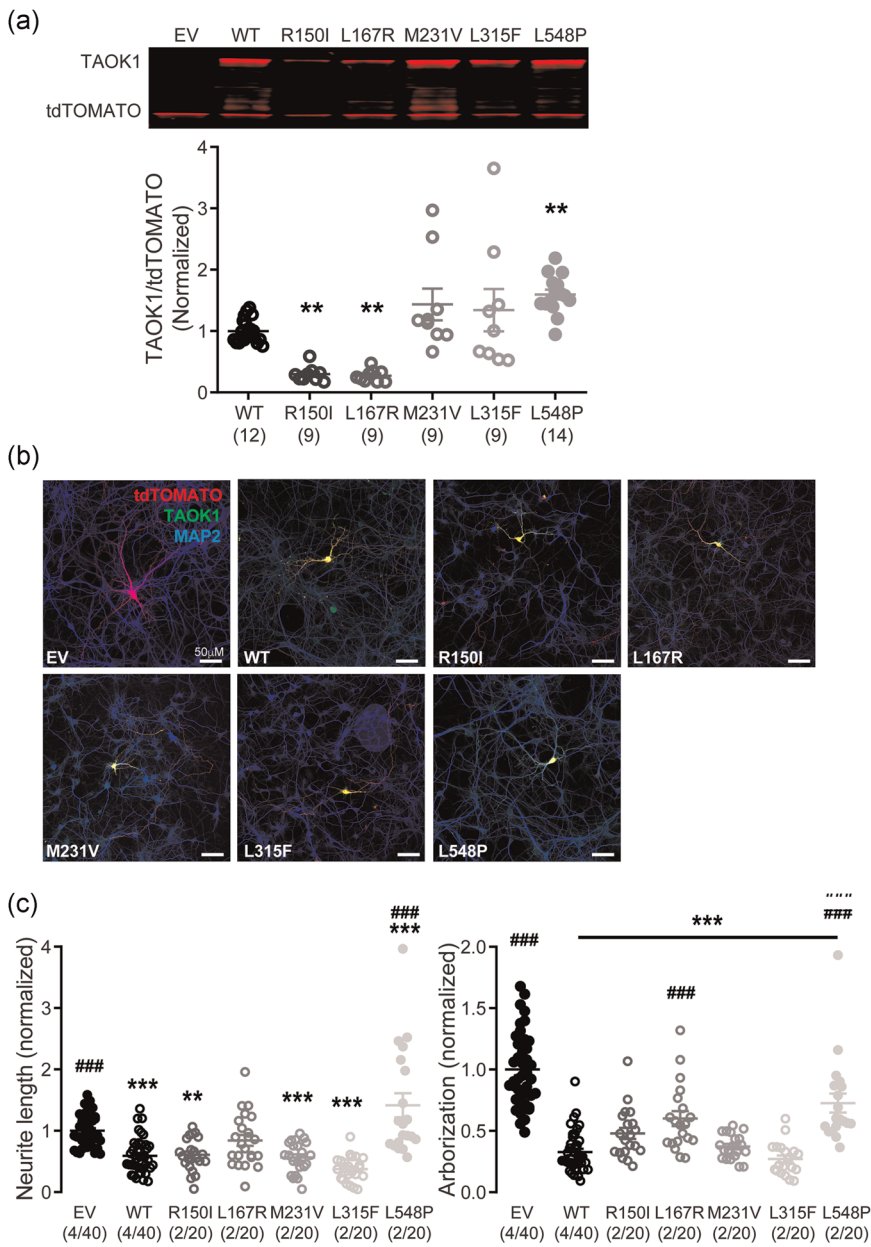


FIGURE 3 Differential effect of TAOK1 variants on protein expression and neuronal development in vitro. (a) Western blot analysis revealing altered expression levels of some TAOK1 variants compared to TAOK1^{WT} when overexpressed in HEK-293T cells. The number of samples is indicated between brackets for each condition. (b) Representative confocal images of hippocampal neurons transfected with empty vector (EV), TAOK1^{WT}, or TAOK1 variants, showing clear overexpression of the TAOK1 protein upon staining for TAOK1 for each TAOK1 condition. (c) Total neurite length and arborization normalized to control. Data are presented as mean ± SEM. The number of independently analyzed culture wells/cells is indicated between brackets for each condition. TAOK1, thousand and one amino-acid kinase 1; WT, wild-type. *Compared to empty vector condition and #compared to TAOK1^{WT} condition. ** $p < .01$, *** $p < .001$, and ### $p < .001$.

used. Transfection of primary hippocampal neurons was performed after growing the neurons for 3 days in vitro (DIV) when the neurons start to form secondary and tertiary branches. Overexpression of $TAOK1^{WT}$ affected neuronal maturation by showing significantly reduced neurite length and arborization compared to the empty vector (EV)-transfected neurons (Figure 3b,c) (Neurite length: one-way ANOVA, $F[6,185] = 18.39$, $p < .0001$; empty vector vs. $TAOK1^{WT}$, $p < .0001$, Dunnett's multiple comparison test; Arborization: one-way ANOVA, $F[6,185] = 38.93$, $p < .0001$; empty vector vs. $TAOK1^{WT}$, $p < .0001$, Dunnett's multiple comparison test). $TAOK1^{Arg150Ile}$, $TAOK1^{Met231Val}$, and $TAOK1^{Leu315phe}$ behaved similarly to $TAOK1^{WT}$ upon overexpression (Neurite length: $TAOK1^{Arg150Ile}$ vs. $TAOK1^{WT}$, $p = .99$; $TAOK1^{Met231Val}$ vs. $TAOK1^{WT}$, $p = .99$; $TAOK1^{Leu315phe}$ vs. $TAOK1^{WT}$, $p = .17$, Dunnett's multiple comparison test; Arborization: $TAOK1^{Arg150Ile}$ vs. $TAOK1^{WT}$, $p = .10$; $TAOK1^{Met231Val}$ vs. $TAOK1^{WT}$, $p = .97$; $TAOK1^{Leu315phe}$ vs. $TAOK1^{WT}$, $p = .91$, Dunnett's multiple comparison test). $TAOK1^{Leu167Arg}$ and $TAOK1^{Leu548Pro}$ showed a milder effect on neuronal development. Neuronal arborization was still significantly decreased upon overexpression of the $TAOK1^{Leu167Arg}$ and $TAOK1^{Leu548Pro}$ variants compared to empty vector, but the effect was not as strong as wild-type $TAOK1$ overexpression as the arborization was significantly higher in $TAOK1^{Leu167Arg}$ and $TAOK1^{Leu548Pro}$ compared to $TAOK1^{WT}$ (empty vector vs.

$TAOK1^{Leu167Arg}$, $p < .0001$; empty vector vs. $TAOK1^{Leu548Pro}$, $p = .0002$; $TAOK1^{Leu167Arg}$ vs. $TAOK1^{WT}$, $p = .0002$; $TAOK1^{Leu548Pro}$ vs. $TAOK1^{WT}$, $p < .0001$, Dunnett's multiple comparison test). The effect on neurite length was in fact for the $TAOK1^{Leu548Pro}$ variant opposite of $TAOK1^{WT}$ overexpression, showing a significantly increased neurite length compared to empty vector and compared to $TAOK1^{WT}$ (empty vector vs. $TAOK1^{Leu548Pro}$, $p = .0009$; $TAOK1^{Leu548Pro}$ vs. $TAOK1^{WT}$, $p < .0001$, Dunnett's multiple comparison test). The $TAOK1^{Leu167Arg}$ variant only partially restored the effect of $TAOK1^{WT}$ on neurite length, revealing a trend, though not significant toward increased neurite length compared to $TAOK1^{WT}$, and showing no significant difference compared to empty vector (empty vector vs. $TAOK1^{Leu167Arg}$, $p = .49$; $TAOK1^{Leu167Arg}$ vs. $TAOK1^{WT}$, $p = .083$, Dunnett's multiple comparison test).

Finally, knowing that the in vivo neuronal migration assay is sensitive to reduced $TAOK1$ function, we evaluated the effect of overexpression of the different $TAOK1$ variants compared to overexpression of $TAOK1^{WT}$ using again the in utero electroporation technique. Similar to the knockdown of $Taok1$, though less severe, overexpression of $TAOK1^{WT}$ resulted in a migration deficit when assessed at P1, with only 70% of the cells reaching the CP compared to 95% in the empty vector condition (Figure 4) (one-way ANOVA, $F[7,67] = 28.66$, $p < .0001$; empty vector vs. $TAOK1^{WT}$: $p = .0011$,

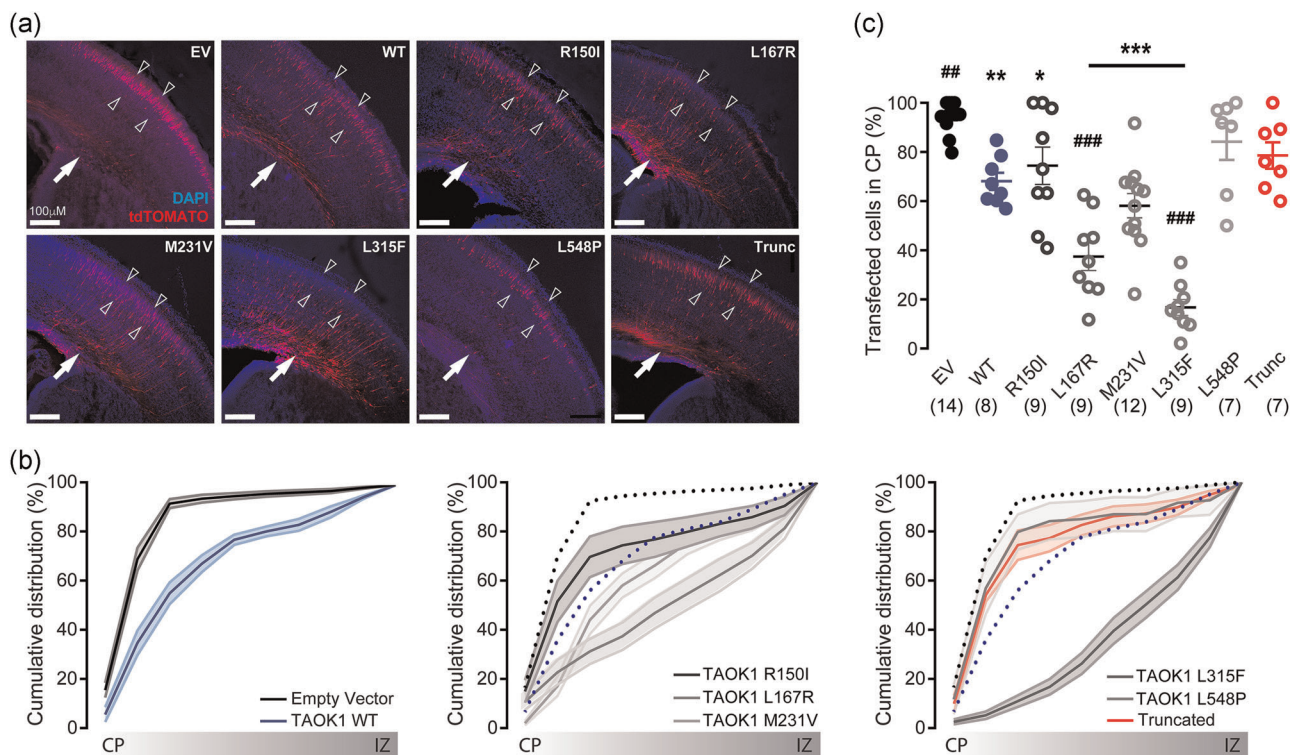


FIGURE 4 Differential effect of thousand and one amino-acid kinase 1 ($TAOK1$) variants on neuronal migration in vivo. (a) Representative images from postnatal Day 1 brain, showing the transfected cells (tdTomato+) from the subventricular zone (SVZ; indicated by the arrow) to the cortical plate (CP; indicated by the arrowheads). (b) Cumulative distribution of the transfected neurons at P1 from the CP to the intermediate zone (IZ). (c) Percentage of neurons reaching the superficial layers of the cortex (sum of bins 1–4). Data are presented as mean \pm SEM. Number of images analyzed is indicated for each condition. *Compared to empty vector condition and #compared to $TAOK1^{WT}$ condition. * $p < .05$, ** $p < .01$, *** $p < .001$, ### $p < .001$, and ### $p < .001$

Dunnnett's multiple comparison test), indicating that the expression level of TAOK1 needs to be well regulated during early neurodevelopment. Interestingly, whereas overexpression of TAOK1^{Leu167Arg} and TAOK1^{Leu315Phe} revealed a stronger migration deficit compared to TAOK1^{WT}, TAOK1^{Leu548Pro} showed normal migration compared to the empty vector condition and a strong trend toward improved migration compared to TAOK1^{WT} (Figure 4, TAOK1^{Leu167Arg} vs. TAOK1^{WT} $p = .0005$; TAOK1^{Leu315Phe} vs. TAOK1^{WT}, $p < .0001$; empty vector vs. TAOK1^{Leu548Pro}: $p = .57$; TAOK1^{WT} vs. TAOK1^{Leu548Pro}: $p = .19$, Dunnnett's multiple comparison test). Overexpression of TAOK1^{Arg150Ile} and TAOK1^{Met231Val} revealed similar migration deficits as seen upon overexpression of TAOK1^{WT} (empty vector vs. TAOK1^{Arg150Ile}, $p = .016$; empty vector vs. TAOK1^{Met231Val}, $p < .0001$; TAOK1^{Arg150Ile} vs. TAOK1^{WT}, $p = .9$; TAOK1^{Met231Val} vs. TAOK1^{WT}, $p = .53$, Dunnnett's multiple comparison test).

To study the effect of truncating variants, we generated a truncated TAOK1, ending at c.2442 (p.Tyr815Ter; TAOK1^{trunc}), and evaluated the effect on migration. Overexpression of TAOK1^{trunc} resulted in an improved migration pattern when compared to empty vector and TAOK1^{WT}, showing no significant difference compared to each of these conditions (empty vector vs. TAOK1^{trunc}: $p = .14$; TAOK1^{WT} vs. TAOK1^{trunc}: $p = .6$, Dunnnett's multiple comparison test), indicating a mild LoF effect.

Taken together, these results show that overexpression of TAOK1^{WT} is damaging for neurons both in vitro and in vivo, and that whereas some variants in TAOK1 behave as LoF variants, others affect the protein in different ways (see Table 3 for a summary of the effects found in the different functional assays), suggesting that TAOK1-related disorder can be caused by distinct pathophysiological mechanisms.

4 | DISCUSSION

With the increased genetic diagnostic yield in cohorts of patients with NDDs, novel genes are found to play an important role in neurodevelopment. Yet, determining the function of these genes and the encoded proteins often lags behind. Of the human TAOK family, so far only for TAOK2, a role in neurodevelopment was shown

(Richter et al., 2018). Recently, eight individuals with NDD carrying de novo variants in TAOK1 were described (Dulovic-Mahlov et al., 2019), but the functional consequences of the TAOK1 missense variants on neuronal function were not assessed. Here, we provide compelling evidence that TAOK1 is important for neuronal function: We show that changing the expression level of TAOK1 (either increasing or decreasing it) in a subset of neural progenitor cells disrupts neural migration, suggesting that the expression level of TAOK1 needs to be regulated for proper neuronal function. In addition, we show that overexpression of TAOK1 affects neuronal maturation in vitro. Moreover, we further delineate the clinical spectrum as well as the molecular mechanisms associated with TAOK1 mutations: (1) The majority of 22 novel individuals carrying different variants in, or deletion of, TAOK1 we identified, had a neurodevelopmental disorder characterized by similar facial features, ID/DD and/or variable learning or behavioral problems, muscular hypotonia, infant feeding difficulties, and growth problems and (2) we show that missense and truncating variants affect TAOK1 protein functioning in different ways, thereby showing that besides haploinsufficiency, also other molecular mechanisms are at play. Unfortunately, patient material was not available, refraining us from testing whether frameshift and nonsense variants result in a truncated protein or whether these mutations induce nonsense-mediated messenger RNA decay.

The eight individuals with de novo variants in TAOK1 that were recently described share common features of global developmental delay, muscular hypotonia, and in the four of eight cases that could be assessed, a formal diagnosis of ID (Dulovic-Mahlov et al., 2019). Here, we describe 20 additional individuals with TAOK1 intragenic variants allowing us to further define the TAOK1-associated disorder. We noted that the global developmental delay might be very mild and that behavior problems and/or overlapping facial features might be the main reason for referral for genetic testing. Other significant features are growth abnormalities (small stature, overweight, and macrocephaly), neonatal feeding difficulties, joint hypermobility, and recurrent ear and airway infections.

Using in vivo and in vitro assays, we have shown that TAOK1 plays an important role in neural development. In our in vitro assay, overexpression of TAOK1 reduces neurite length and arborization in

TABLE 3 Overview of functional assessment of TAOK1 missense variants

	Protein expression compared to WT TAOK1	Neuronal morphology compared to WT TAOK1	Neuronal migration compared to WT TAOK1	Inferred pathophysiological mechanism
Empty vector		Increased complexity	Increased	
p.Arg150Ile	Reduced	Similar	Similar	Loss of Function
p.Leu167Arg	Reduced	Increased complexity	Severely impaired	Dominant acting
p.Met231Val	Unaffected	Similar	Similar	None
p.Leu315Phe	Unaffected	Similar	Severely impaired	Dominant acting
p.Leu548Pro	Increased	Increased complexity	Increased	Loss of Function

Abbreviations: TAOK1, thousand and one amino-acid kinase 1; WT, wild-type.

mouse primary hippocampal neurons. This seems to contrast to earlier findings, showing that in differentiating PC12 cells, TAOK1 is required for neurite outgrowth as the absence of TAOK1 severely reduces the number of differentiating neurons with neurites (Timm et al., 2003). However, it should be noted that we induce the overexpression of TAOK1 from DIV3, which is after the initiation of neurite outgrowth (Dotti et al., 1988). Additionally, we are using a different neuronal population (primary hippocampal neurons) and do not induce neuronal differentiation. Finally, overexpression might affect different pathways compared to knockdown.

Of the TAOK1 variants tested, TAOK1^{Arg150Ile} and TAOK1^{Leu167Arg}, both located in the kinase domain of the protein, showed reduced protein expression in HEK293T cells, which could indicate a LoF mutation. In the functional assays, we observed no difference between the TAOK1^{Arg150Ile} and TAOK1^{WT}, which could indicate that the function of TAOK1^{Arg150Ile} is reduced but potentially can be compensated for by overexpression. TAOK1^{Leu167Arg} does behave differently compared to TAOK1^{WT} in the functional assays, showing a partial rescue of the neuronal morphology phenotype, but a much more severe migration deficit compared to TAOK1^{WT}. These results could suggest that the TAOK1^{Leu167Arg} mutation acts in a dominant acting manner. The TAOK1^{Met231Val} variant is also located in the kinase domain and behaves in all the assays similar to TAOK1^{WT}. Therefore, based on our functional data no conclusions can be drawn with respect to the pathogenicity of this variant. Additionally, for this patient (patient 21), the inheritance is unknown and the phenotype is not specific. It, therefore, remains unclear whether this variant is the (major) cause for the NDD phenotype seen in this individual.

TAOK1^{Leu315Phe} is located in the substrate-binding domain and does not affect expression levels nor neuronal morphology. Interestingly, this variant does severely affect the *in vivo* migration of neurons when overexpressed, therefore, likely having a dominant-negative effect on TAOK1 function. The TAOK1^{Leu548Pro} variant yielded increased protein expression levels, improved neuronal morphology *in vitro* as well as improved neuronal migration *in vivo* compared to TAOK1^{WT}, indicating an LoF effect on TAOK1. Together these results reveal that dysregulation of TAOK1 in several ways might result in a neurodevelopmental disorder.

The precise TAOK1 downstream signaling pathways responsible for the neurodevelopmental deficits remain to be elucidated, as literature on the role of TAOK1 in the brain is limited. Most data come from studies in *Drosophila melanogaster*, which has a single TAOK ortholog, called *Tao*. *Tao1* in *Drosophila* plays a role in axon guidance, and its deletion leads to malformations of the fly brain (Dulovic-Mahlow et al., 2019; King et al., 2011; Poon et al., 2016). It is hypothesized that this is the result of dysregulation of the Par-1/Tau pathway, which affects the microtubule dynamics in developing neurons (King & Heberlein, 2011). However, as *Drosophila* has only one representative gene (*Tao1*) for the TAOK family, whereas humans have three TAOK genes, it is difficult to translate findings of *Tao1* knockdown in *Drosophila* to the role of TAOK1 in mammals. Moreover, the regulation of Par-1 by TAOK1 appears to be opposite

when comparing the *Drosophila* with mammalian neurons. In *Drosophila*, Par-1 is thought to be negatively regulated by Tao1 (Wang et al., 2007), whereas in mammalian neurons (PC12 cells differentiated with NGF), TAOK1 was shown to stimulate PAR-1, which leads to phosphorylation of Tau, followed by microtubule dynamics required for neurite outgrowth (Biernat et al., 2002; Timm et al., 2003). Thus, future studies will have to unravel the precise mechanism through which TAOK1 causes NDD.

Taken together, our data show that TAOK1 plays an important role in mammalian neuronal maturation and that dysregulation of TAOK1 either through haploinsufficiency, dominant-negative effects, or even other mechanisms, causes a neurodevelopmental disorder characterized by similar facial features, ID/DD, and/or variable learning or behavioral problems, muscular hypotonia, infant feeding difficulties, and growth problems.

ACKNOWLEDGMENTS

The authors would like to thank the participating families. We thank all clinicians involved for referring individuals with ID for diagnostic exome sequencing and Dr. Simon McGowan for bioinformatics analysis. This study was supported by the Netherlands Organization for Health Research and Development (ZonMw grant 91718310 to T. K.) and by the National Institute for Health Research (NIHR) Oxford Biomedical Research Centre Programme (AOMW). Additionally, this project has received funding from the European Union's Horizon 2020 RESEARCH and INNOVATION PROGRAM under grant agreement No. 779257 (Solve-RD).

CONFLICT OF INTERESTS

Mari Rossi is employed by and receives a salary from Ambry Genetics, one of whose commercially available tests is exome sequencing. Amanda Noyes, Katherine G. Langley, Alice Brooks, Jennifer Humberson, Maria J. Guillen Sacoto, Jane Juusola, Kristin G. Monaghan, and Sumit Punj are employees of GeneDx, Inc.

AUTHOR CONTRIBUTIONS


Geeske M. van Woerden, Ype Elgersma, and Tjitske Kleefstra designed the study. Karen W. Gripp identified a patient and initiated the collaboration through Genematcher. Melanie Bos and Tjitske Kleefstra performed clinical cohort analyses. Geeske M. van Woerden, Rossella Avagliano Trezza, Charlotte de Konink, Fatima Rehman, Saskia Brulleman, Róisín McCormack, and Gwynna de Geus performed functional experiments and analysis. Ben Distel performed the *in silico* modeling. GeneDx: Amanda Noyes and Katherine G. Langley, performed case identification and data collection; Aida Telegrafi, Amy Blevins, Jessica Hoffman, Maria J. Guillen Sacoto, Jane Juusola, Kristin G. Monaghan, and Sumit Punj performed analysis and reporting of GeneDx cases. Eduardo Calpena and Andrew O.M. Wilkie identified an additional case by exome sequencing. Natasha E. Shur, Kristin Barañano, Sonal Mahida, Anna Chassevent, Arthur Sorlin, Ange-Line Bruel, Angelika L. Erwin, Karen W. Gripp, Louisa Kalsner, Allison Schreiber, Alice Brooks, Marjon van

Selgtenhorst, David A. Koolen, Melissa K. Gabriel, Mari Rossi, David R. Fitzpatrick, Andrew O.M. Wilkie, Eduardo Calpena, David Johnson, Julie Fleischer, Daniel Groepper, Kristin Lindstrom, A. Micheil Innes, Marleen Simon, Allison Goodwin, Jennifer Humberson, and Rolf Pfundt contributed to the clinical information of patients and reviewed the manuscript. Geeske M. van Woerden, Ype Elgersma, Melanie Bos, and Tjitske Kleefstra drafted the manuscript. All authors contributed to the final version of the manuscript.

DATA AVAILABILITY STATEMENT

All data are available upon request. Accession number used for cloning the human TAOK1: NM_020791.2, https://www.ncbi.nlm.nih.gov/nuccore/NM_020791.2.

ORCID

Geeske M. van Woerden  <https://orcid.org/0000-0003-2492-9239>
 Melanie Bos  <https://orcid.org/0000-0003-1833-786X>
 Ben Distel  <https://orcid.org/0000-0002-3046-205X>
 Rossella Avagliano Trezza  <https://orcid.org/0000-0002-1857-5449>
 Angelika L. Erwin  <https://orcid.org/0000-0002-8791-0554>
 Róisín McCormack  <https://orcid.org/0000-0002-8356-9950>
 Gwynna de Geus  <https://orcid.org/0000-0002-2000-3298>
 Arthur Sorlin  <https://orcid.org/0000-0001-8008-9145>
 Ange-Line Bruel  <http://orcid.org/0000-0002-0526-465X>
 Andrew O.M. Wilkie  <https://orcid.org/0000-0002-2972-5481>
 Eduardo Calpena  <https://orcid.org/0000-0001-6399-6528>
 A. Micheil Innes  <https://orcid.org/0000-0001-9881-5467>
 Ype Elgersma  <https://orcid.org/0000-0002-3758-1297>

REFERENCES

- Biernat, J., Wu, Y.-Z., Timm, T., Zheng-Fischhöfer, Q., Mandelkow, E., Meijer, L., & Mandelkow, E.-M. (2002). Protein kinase MARK/PAR-1 is required for neurite outgrowth and establishment of neuronal polarity. *Molecular Biology of the Cell*, 13(11), 4013–4028. <https://doi.org/10.1091/mbc.02-03-0046>
- Dan, I., Watanabe, N. M., & Kusumi, A. (2001). The Ste20 group kinases as regulators of MAP kinase cascades. *Trends in Cell Biology*, 11(5), 220–230.
- Deciphering Developmental Disorders Study. (2017). Prevalence and architecture of de novo mutations in developmental disorders. *Nature*, 542(7642), 433–438. <https://doi.org/10.1038/nature21062>
- Dotti, C. G., Sullivan, C. A., & Banker, G. A. (1988). The establishment of polarity by hippocampal neurons in culture. *The Journal of Neuroscience: The Official Journal of the Society for Neuroscience*, 8(4), 1454–1468.
- Draviam, V. M., Stegmeier, F., Nalepa, G., Sowa, M. E., Chen, J., Liang, A., Hannon, G. J., Sorger, P. K., Harper, J. W., & Elledge, S. J. (2007). A functional genomic screen identifies a role for TAO1 kinase in spindle-checkpoint signalling. *Nature Cell Biology*, 9(5), 556–564. <https://doi.org/10.1038/ncb1569>
- Dulovic-Mahlow, M., Trinh, J., Kandaswamy, K. K., Braathen, G. J., Di Donato, N., Rahikkala, E., Beblo, S., Werber, M., Krajka, V., Busk, Ø. L., Baumann, H., Al-Sanna, N. A., Hinrichs, F., Affan, R., Navot, N., Al Balwi, M. A., Oprea, G., Holla, Ø. L., Weiss, M. E. R., ... Lohmann, K. (2019). De novo variants in TAOK1 cause neurodevelopmental disorders. *American Journal of Human Genetics*, 105, 213–220. <https://doi.org/10.1016/j.ajhg.2019.05.005>
- Farwell, K. D., Shahmirzadi, L., El-Khechen, D., Powis, Z., Chao, E. C., Tippin Davis, B., Baxter, R. M., Zeng, W., Mroske, C., Parra, M. C., Gandomi, S. K., Lu, I., Li, X., Lu, H., Lu, H. M., Salvador, D., Ruble, D., Lao, M., Fischbach, S., ... Tang, S. (2014). Enhanced utility of family-centered diagnostic exome sequencing with inheritance model-based analysis: Results from 500 unselected families with undiagnosed genetic conditions. *Genetics in Medicine*, 17(7), 578–586. <https://doi.org/10.1038/gim.2014.154>
- Farwell Hagman, K. D., Shinde, D. N., Mroske, C., Smith, E., Radtke, K., Shahmirzadi, L., El-Khechen, D., Powis, Z., Chao, E. C., Alcaraz, W. A., Helbig, K. L., Sajan, S. A., Rossi, M., Lu, H. M., Huether, R., Li, S., Wu, S., Nuñez, M. E., & Tang, S. (2016). Candidate-gene criteria for clinical reporting: diagnostic exome sequencing identifies altered candidate genes among 8% of patients with undiagnosed diseases. *Genetics in Medicine*, 19(2), 224–235. <https://doi.org/10.1038/gim.2016.95>
- Goslin, K., & Banker, G. (1991). *Culturing Nerve Cells*. MIT Press.
- Gurovich, Y., Hanani, Y., Bar, O., Nadav, G., Fleischer, N., Gelbman, D., Basel-Salmon, L., Krawitz, P. M., Kamphausen, S. B., Zenker, M., Bird, L. M., & Gripp, K. W. (2019). Identifying facial phenotypes of genetic disorders using deep learning. *Nature Medicine*, 25(1), 60–64. <https://doi.org/10.1038/s41591-018-0279-0>
- Hutchison, M., Berman, K. S., & Cobb, M. H. (1998). Isolation of TAO1, a protein kinase that activates MEKs in stress-activated protein kinase cascades. *The Journal of Biological Chemistry*, 273(44), 28625–28632.
- Kehrer-Sawatzki, H., Mautner, V.-F., & Cooper, D. N. (2017). Emerging genotype-phenotype relationships in patients with large NF1 deletions. *Human Genetics*, 136(4), 349–376. <https://doi.org/10.1007/s00439-017-1766-y>
- King, I., & Heberlein, U. (2011). Tao kinases as coordinators of actin and microtubule dynamics in developing neurons. *Communicative & Integrative Biology*, 4(5), 554–556. <https://doi.org/10.4161/cib.4.5.16051>
- King, I., Tsai, L. T.-Y., Pflanz, R., Voigt, A., Lee, S., Jackle, H., Lu, B., & Heberlein, U. (2011). Drosophila tao controls mushroom body development and ethanol-stimulated behavior through par-1. *Journal of Neuroscience*, 31(3), 1139–1148. <https://doi.org/10.1523/JNEUROSCI.4416-10.2011>
- Küry, S., van Woerden, G. M., Besnard, T., Proietti Onori, M., Latypova, X., Towne, M. C., Cho, M. T., Prescott, T. E., Ploeg, M. A., Sanders, S., Stessman, H. A. F., Pujol, A., Distel, B., Robak, L. A., Bernstein, J. A., Denommé-Pichon, A. S., Lesca, G., Sellars, E. A., Berg, J., ... Mercier, S. (2017). De novo mutations in protein kinase genes CAMK2A and CAMK2B cause intellectual disability. *American Journal of Human Genetics*, 101(5), 768–788. <https://doi.org/10.1016/j.ajhg.2017.10.003>
- Lelieveld, S. H., Reijnders, M. R. F., Pfundt, R., Yntema, H. G., Kamsteeg, E.-J., de Vries, P., de Vries, B. B. A., Willemsen, M. H., Kleefstra, T., Löhner, K., Vreeburg, M., Stevens, S. J. C., van der Burgt, I., Bongers, E. M. H. F., Stegmann, A. P. A., Rump, P., Rinne, T., Nelen, M. R., Veltman, J. A., ... Gilissen, C. (2016). Meta-analysis of 2, 104 trios provides support for 10 new genes for intellectual disability. *Nature Neuroscience*, 19(9), 1194–1196. <https://doi.org/10.1038/nn.4352>
- Poon, C. L. C., Mitchell, K. A., Kondo, S., Cheng, L. Y., & Harvey, K. F. (2016). The Hippo pathway regulates neuroblasts and brain size in *Drosophila melanogaster*. *Current Biology*, 26(8), 1034–1042. <https://doi.org/10.1016/j.cub.2016.02.009>
- Proietti Onori, M., Koopal, B., Everman, D. B., Worthington, J. D., Jones, J. R., Ploeg, M. A., Mientjes, E., van Bon, B. W., Kleefstra, T., Schulman, H., Kushner, S. A., Küry, S., Elgersma, Y., & van Woerden, G. M. (2018). The intellectual disability-associated CAMK2G p.Arg292Pro mutation acts as a pathogenic gain-of-

- function. *Human Mutation*, 39(12), 2008–2024. <https://doi.org/10.1002/humu.23647>
- Pucilowska, J., Vithayathil, J., Tavares, E. J., Kelly, C., Karlo, J. C., & Landreth, G. E. (2015). The 16p11.2 deletion mouse model of autism exhibits altered cortical progenitor proliferation and brain cytoarchitecture linked to the ERK MAPK pathway. *Journal of Neuroscience*, 35(7), 3190–3200. <https://doi.org/10.1523/JNEUROSCI.4864-13.2015>
- Raman, M., Earnest, S., Zhang, K., Zhao, Y., & Cobb, M. H. (2007). TAO kinases mediate activation of p38 in response to DNA damage. *The EMBO Journal*, 26(8), 2005–2014. <https://doi.org/10.1038/sj.emboj.7601668>
- Reijnders, M. R. F., Kousi, M., van Woerden, G. M., Klein, M., Bralten, J., Mancini, G. M. S., van Essen, T., Proietti-Onori, M., Smeets, E. E. J., van Gastel, M., Stegmann, A. P. A., Stevens, S. J. C., Lelieveld, S. H., Gilissen, C., Pfundt, R., Tan, P. L., Kleefstra, T., Franke, B., Elgersma, Y., ... Brunner, H. G. (2017). Variation in a range of mTOR-related genes associates with intracranial volume and intellectual disability. *Nature Communications*, 8(1), 1052. <https://doi.org/10.1038/s41467-017-00933-6>
- Retterer, K., Juusola, J., Cho, M. T., Vitazka, P., Millan, F., Gibellini, F., Vertino-Bell, A., Smaoui, N., Neidich, J., Monaghan, K. G., McKnight, D., Bai, R., Suchy, S., Friedman, B., Tahiliani, J., Pineda-Alvarez, D., Richard, G., Brandt, T., Haverfield, E., ... Bale, S. (2015). Clinical application of whole-exome sequencing across clinical indications. *Genetics in Medicine*, 18(7), 696–704. <https://doi.org/10.1038/gim.2015.148>
- Richter, M., Murtaza, N., Scharrenberg, R., White, S. H., Johanns, O., Walker, S., et al. (2018). Altered TAO2 activity causes autism-related neurodevelopmental and cognitive abnormalities through RhoA signaling. *Molecular Psychiatry*, 20(Pt 6), 1237. <https://doi.org/10.1038/s41380-018-0025-5>
- Saito, T., & Nakatsuji, N. (2001). Efficient gene transfer into the embryonic mouse brain using in vivo electroporation. *Developmental Biology*, 240(1), 237–246. <https://doi.org/10.1006/dbio.2001.0439>
- Sobreira, N., Schiettecatte, F., Valle, D., & Hamosh, A. (2015). GeneMatcher: a matching tool for connecting investigators with an interest in the same gene. *Human Mutation*, 36(10), 928–930. <https://doi.org/10.1002/humu.22844>
- Tabata, H., & Nakajima, K. (2001). Efficient in utero gene transfer system to the developing mouse brain using electroporation: visualization of neuronal migration in the developing cortex. *Nsc*, 103(4), 865–872.
- Taniguchi, Y., Young-Pearse, T., Sawa, A., & Kamiya, A. (2012). In utero electroporation as a tool for genetic manipulation in vivo to study psychiatric disorders: From genes to circuits and behaviors. *The Neuroscientist*, 18(2), 169–179. <https://doi.org/10.1177/1073858411399925>
- Timm, T., Li, X.-Y., Biernat, J., Jiao, J., Mandelkow, E., Vandekerckhove, J., & Mandelkow, E.-M. (2003). MARKK, a Ste20-like kinase, activates the polarity-inducing kinase MARK/PAK-1. *The EMBO Journal*, 22(19), 5090–5101. <https://doi.org/10.1093/emboj/cdg447>
- Twigg, S. R. F., Forecki, J., Goos, J. A. C., Richardson, I. C. A., Hoogeboom, A. J. M., van den Ouweland, A. M. W., Swagemakers, S. M. A., Lequin, M. H., van Antwerp, D., McGowan, S. J., Westbury, I., Miller, K. A., Wall, S. A., van der Spek, P. J., Mathijssen, I. M. J., Pauws, E., Merzdorf, C. S., & Wilkie, A. O. M. (2015). Gain-of-function mutations in ZIC1 are associated with coronal craniosynostosis and learning disability. *American Journal of Human Genetics*, 97(3), 378–388. <https://doi.org/10.1016/j.ajhg.2015.07.007>
- Wang, J.-W., Imai, Y., & Lu, B. (2007). Activation of PAR-1 kinase and stimulation of tau phosphorylation by diverse signals require the tumor suppressor protein LKB1. *Journal of Neuroscience*, 27(3), 574–581. <https://doi.org/10.1523/JNEUROSCI.5094-06.2007>
- Weiss, K., Terhal, P. A., Cohen, L., Bruccoleri, M., Irving, M., Martinez, A. F., Rosenfeld, J. A., Machol, K., Yang, Y., Liu, P., Walkiewicz, M., Beuten, J., Gomez-Ospina, N., Haude, K., Fong, C. T., Enns, G. M., Bernstein, J. A., Fan, J., Gotway, G., ... Muenke, M. (2016). De novo mutations in CHD4, an ATP-dependent chromatin remodeler gene, cause an intellectual disability syndrome with distinctive dysmorphisms. *American Journal of Human Genetics*, 99(4), 934–941. <https://doi.org/10.1016/j.ajhg.2016.08.001>
- Weiss, L. A., Shen, Y., Korn, J. M., Arking, D. E., Miller, D. T., Fossdal, R., Saemundsen, E., Stefansson, H., Ferreira, M. A. R., Green, T., Platt, O. S., Ruderfer, D. M., Walsh, C. A., Altshuler, D., Chakravarti, A., Tanzi, R. E., Stefansson, K., Santangelo, S. L., Gusella, J. F., ... Daly, M. J. (2008). Association between microdeletion and microduplication at 16p11.2 and autism. *The New England Journal of Medicine*, 358(7), 667–675. <https://doi.org/10.1056/NEJMoa075974>
- Wright, C. F., McRae, J. F., Clayton, S., Gallone, G., Aitken, S., Fitzgerald, T. W., Jones, P., Prigmore, E., Rajan, D., Lord, J., Sifrim, A., Kelsell, R., Parker, M. J., Barrett, J. C., Hurler, M. E., FitzPatrick, D. R., & Firth, H. V. (2018). Making new genetic diagnoses with old data: Iterative reanalysis and reporting from genome-wide data in 1,133 families with developmental disorders. *Genetics in Medicine*, 20(10), 1216–1223. <https://doi.org/10.1038/gim.2017.246>
- Xie, B., Fan, X., Lei, Y., Chen, R., Wang, J., Fu, C., Yi, S., Luo, J., Zhang, S., Yang, Q., Chen, S., & Shen, Y. (2016). A novel de novo microdeletion at 17q11.2 adjacent to NF1 gene associated with developmental delay, short stature, microcephaly and dysmorphic features. *Molecular Cytogenetics*, 9(1), 41. <https://doi.org/10.1186/s13039-016-0251-y>
- Yang, J., & Zhang, Y. (2015). I-TASSER server: New development for protein structure and function predictions. *Nucleic Acids Research*, 43(W1), W174–81. <https://doi.org/10.1093/nar/gkv342>
- Zhang, Z., Tang, Z., Ma, X., Sun, K., Fan, L., Fang, J., Pan, J., Wang, X., An, H., & Zhou, J. (2018). TAO1 negatively regulates IL-17-mediated signaling and inflammation. *Cellular & Molecular Immunology*, 15(8), 794–802. <https://doi.org/10.1038/cmi.2017.158>
- Zihni, C., Mitsopoulos, C., Tavares, I. A., Ridley, A. J., & Morris, J. D. H. (2006). Prostate-derived sterile 20-like kinase 2 (PSK2) regulates apoptotic morphology via c-Jun N-terminal kinase and Rho kinase-1. *The Journal of Biological Chemistry*, 281(11), 7317–7323. <https://doi.org/10.1074/jbc.M513769200>

SUPPORTING INFORMATION

Additional Supporting Information may be found online in the supporting information tab for this article.

How to cite this article: van Woerden, G. M., Bos, M., de Konink, C., et al. (2021). TAO1 is associated with neurodevelopmental disorder and essential for neuronal maturation and cortical development. *Human Mutation*, 42, 445–459. <https://doi.org/10.1002/humu.24176>